Experimental and Theoretical Study of Twin-Screw Extrusion of Polypropylene

O. S. CARNEIRO,[1] J. A. COVAS,[1] B. VERGNES[2]

[1] Department of Polymer Engineering, University of Minho, Campus de Azurém, 4800 Guimaraes, Portugal

[2] CEMEF, Ecole des Mines de Paris, UMR CNRS 7635, BP 207, 06904 Sophia-Antipolis Cedex, France

Received 9 November 1999; accepted 29 March 2000

ABSTRACT: The flow of a polypropylene in a self-wiping corotating twin-screw extruder was characterized by measuring the pressure, temperature, and residence time along the screw profile. The influence of the operating conditions (feed rate, screw speed, barrel temperature) and screw profile was studied. Flow modeling was performed using the Ludovic© software and measured and calculated pressure, temperature, residence time, and energy consumption were compared. The values of the temperature close to the melting zone were overestimated by the model, which considers instantaneous melting upon the first restrictive screw element. If the program assumes that melting occurs at the screw location identified experimentally, a correct description of the temperatures along the screw profile is produced. The influence of the processing conditions (feed rate, screw speed, barrel temperature, screw profile) is well described by the model. These results put in evidence the importance of including an adequate melting model in the modeling of the twin-screw extrusion process. © 2000 John Wiley & Sons, Inc. J Appl Polym Sci 78: 1419–1430, 2000

Key words: twin-screw extrusion; polypropylene; temperature measurement; modeling

INTRODUCTION

Twin-screw extrusion has been used extensively by the polymer industry in various applications, including mixing, compounding, and reactive extrusion.[1,2] Among the various available system configurations, corotating self-wiping screws have gained wide acceptance, due to their good balance between mixing efficiency and pressure-generation capacity. Process engineering and optimization requires the knowledge of the values of the main-flow parameters (e.g., pressure, temperature, residence time, shear rate, specific energy) at different locations along the screw profile and how they are influenced by variables such as screw geometry, feed rate, screw speed, or barrel temperature.

Numerous experimental studies on twin-screw extrusion have been reported in the literature. Their relevance is related to the reliability of the technique used to measure the process parameters, to the practical importance of the variables monitored, and to the location of the sensors in the extruder. Global residence time distribution functions are relatively easy to obtain; they are calculated from the variation with time of the concentration of a tracer that can be detected using different techniques such as fluorescence emission,[3,4] solids residual weight measurement,[5] ultrasonic attenuation,[6] or light absorption.[7] Melt-pressure measurements are possible in the filled sections of the screw or in blocks of kneading discs.[8,9] Local material

Correspondence to: B. Vergnes.

Contract grant sponsors: ICCTI (Portugal); Ambassade de France (Portugal).

Journal of Applied Polymer Science, Vol. 78, 1419–1430 (2000)

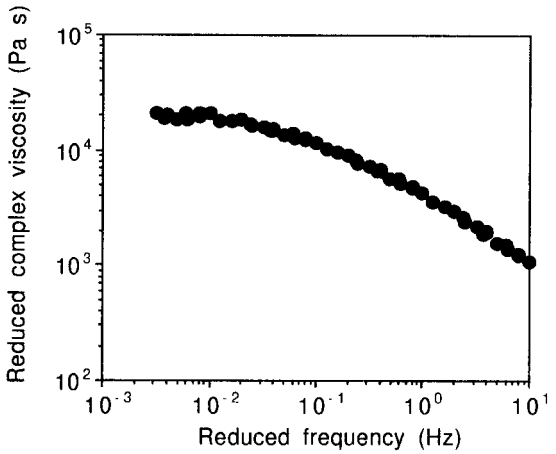

Figure 1 Complex viscosity master curve at 200°C.

temperature is another important parameter, but more difficult to measure with accuracy. Flush-mounted thermocouples measure the melt temperature at the wall; for reliable measurements, protruding probes insulated from the barrel wall are recommended (although they affect the local velocity field and, consequently, the actual melt temperatures). Infrared probes appear as an interesting technique, as it allows measurements along the screw channel.[10,11] However, the technique has some limitations since measurements are carried out on the melt surface or in the bulk, depending on the melt emissivity.[10] Furthermore, measurements performed in partially filled sections are not accurate.[10]

In this work, measurements of pressure, melt temperature, residence time, and energy consumption were carried out on a laboratory-scale twin-screw extruder. The use of sampling devices developed by Machado et al.[12] allowed us to perform these measurements at six different locations along the extruder.

Knowledge of the extrusion process can also be gathered through numerical simulation. Recent developments provided descriptions of the three-dimensional flow field in filled screw elements[13,14] and in blocks of kneading discs.[15,16] Global (plasticating) models, taking into account the whole history of the extruded material from the hopper to the die exit, have also been published.[17–20] In the present study of such a global model, the software Ludovic© was used to predict the flow conditions along the extruder. The direct comparison between measured and computed values is important for assessing the theoretical model and may suggest relevant modifications that may improve the accuracy of its predictions.

PROCEDURE

Polymer

The experiments were performed using a polypropylene homopolymer (HB121J, from Borealis,

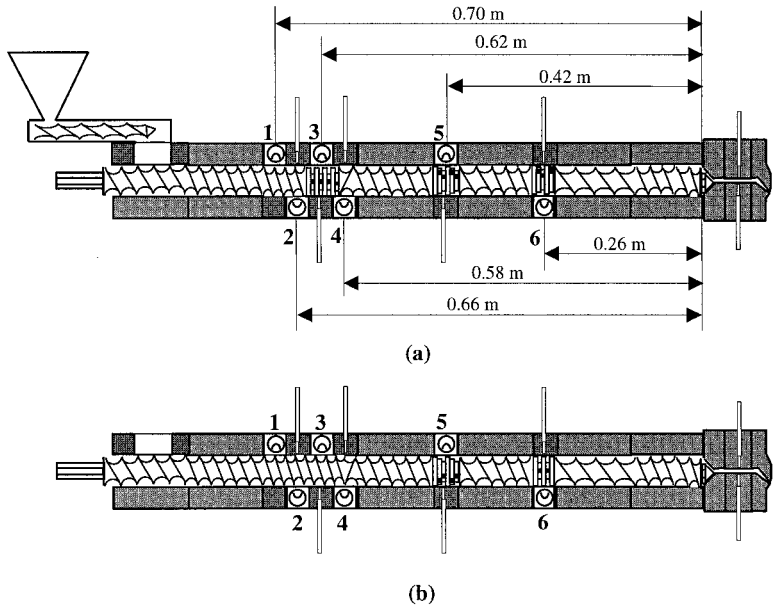

Figure 2 Screw profiles (a) A and (b) B and location of the sampling devices (ports 1–6).

Table I Screw Profile A, From Hopper to Die

	Length (mm)												
Parameter	97.5	150	60	60	30	120	45	60	60	37.5	120	90	30
Pitch (mm)	45	30	20	KD90	−30	30	KD−60	45	30	KD−30	60	30	20

A negative pitch indicates a left-handed element; KD −30 denotes a block of left-handed kneading discs, with a staggering angle of 30°.

Lyngby, Denmark). It has a density of 902 kg m^{-3} and a melt-flow index of 1.9 g/10 min (ISO 1133: 230°C, 2.16 kg). Its rheological behavior was measured in small amplitude oscillatory shear (Rheometrics RMS 800) at three temperatures (200, 220, and 240°C). The complex viscosity master curve of this resin is presented in Figure 1. We assumed that the Cox–Merz rule is satisfied and that the viscous behavior is adequately described using a Carreau–Yasuda law:

$$\eta = \eta_0 a_T [1 + (\lambda \dot{\gamma} a_T)^a]^{(n-1)/a} \quad (1)$$

with

$$a_T = \exp[E/R(1/T - 1/T_0)] \quad (2)$$

where the parameters assume the following values: η_0 = 22200 Pa s, λ = 1.7 s, n = 0.35, a = 0.73, E/R = 5546 K, T_0 = 473 K.

Twin-Screw Extrusion

The experiments were carried out on a Leistritz LSM 30.34 corotating intermeshing twin-screw extruder. The screw profile (A) used for the main part of the experimental work is presented in Figure 2(a) and explicitly described in Table I. A second less restrictive profile (B) was used for one operating condition. Its characteristics are given in Table II and Figure 2(b).

The main screw profile includes conveying elements, different types of kneading blocks with staggering angles of 30 and 60° (left-handed) and 90° (neutral), and a left-handed element located after the first block of kneading discs. Six sampling devices are located in the melting and mixing sections [ports 1–6 in Fig. 2(a)]. In the second profile, the melting section is restricted to one left-handed screw element, and all the mixing discs have either positive or neutral staggering. Consequently, this profile is assumed to be less severe than is the first one. The location of the collection ports remained unchanged.

The sampling devices were developed by Machado et al.[12] They allow one not only to measure local pressures and temperatures with PT transducers, but also to collect in a few seconds polymer samples for, for example, temperature measurement, determination of residence time, and evolution of plastication. Originally, they were designed to collect samples from reactive systems that were quenched in liquid nitrogen and characterized subsquentially. The working principle of the device is presented in Figure 3. A circular aperture in the barrel wall (1) allows the pressure flow of material out of the extruder. The occurrence of this flow is controlled by the cylindrical valve (2), containing cavities (3) and (4). When the valve is positioned as shown in the figure, there is no flow out of the barrel. To collect a representative portion of material from inside the extruder, the valve is rotated sequentially to expose hole (1) to cavity (3) where the accumulated material can be discarded and, upon further

Table II Screw Profile B, From Hopper to Die

	Length (mm)											
Parameter	97.5	150	120	30	120	45	60	60	37.5	120	90	30
Pitch (mm)	45	30	20	−30	30	KD60	45	30	KD90	60	30	20

Same legend as in Table I; location of collecting ports is the same.

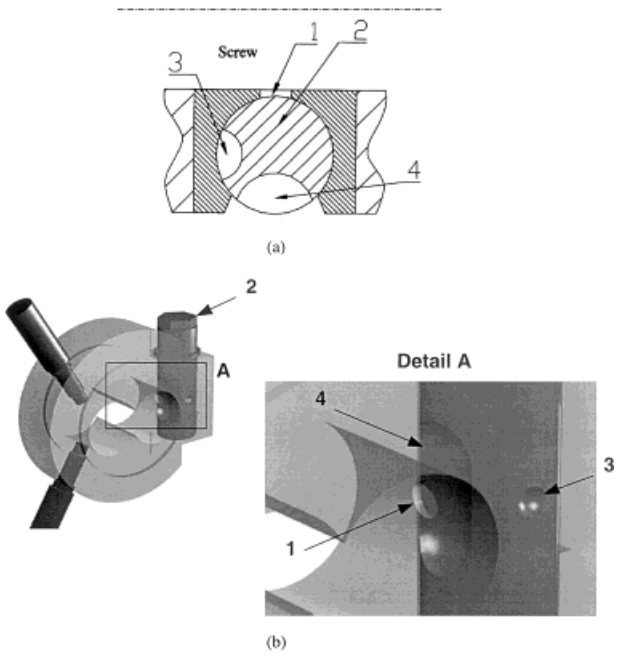

Figure 3 Sampling device: (a) working concept; (b) schematic.

rotation, hole (1) is now exposed to cavity (4), which is rapidly filled with fresh material. The valve is rotated again to the position shown in the figure, where about 1 g of the sample can be removed for subsequent analysis.

Pressures along the extruder and at the die entrance were monitored using flush-mounted Dynisco-type PT transducers connected to a PC interface. Temperatures were measured with the same flush-mounted PT transducers (at locations 2–5) and also by immediately sticking a fast-response thermocouple into the samples collected with the devices (at ports 2–6) and at the extrudate emerging from the die. The average residence time was determined for two runs at three locations (ports 4 and 6 and die exit). Two grams of a powder silica tracer (Degussa Ultrasil VN3) were fed through the hopper throat. Samples were collected in one specific port every 5 s. The tracer concentration was inferred from the weight of the calcinated samples. The average residence time, $\bar{t}$, was computed from[21]

$$\bar{t} = \frac{\sum_0^\infty tC\Delta t}{\sum_0^\infty C\Delta t} \tag{3}$$

where C is the concentration of the tracer at time t, and Δt, the time interval.

The feed rate Q (6, 12, and 18 kg/h), the rotation speed N (100, 150, and 200 rpm), and the barrel temperature T_b (190, 210, and 230°C) were varied. For each run, we measured the motor current (to estimate the mechanical power consumption), the pressure at ports 2–6 (no pressure buildup was observed at port 1) and in the die, and the temperature at the same locations, both in the flow (PT transducer) and in the collected samples. The operating conditions used in the various runs and the corresponding experimentally measured parameters are reported in Tables III and IV, respectively.

Software

Various theoretical approaches to the flow of a molten polymer in a twin-screw extruder may be found in the literature. However, here we are interested in a global plasticating model able to describe the extrusion process from the hopper to the die. Such models have been proposed previ-

Table III Operating Conditions Used in Extrusion Experiments

Run	Screw Configuration	Feed Rate (kg/h)	Screw Speed (rpm)	Barrel Set Temperature (°C)
1	A	12	150	190
2	A	12	150	230
3	A	12	150	210
4	A	12	100	210
5	A	12	200	210
6	A	6	150	210
7	A	18	150	210
8	B	12	150	210

Table IV Measured Extruder Motor Currenty Intensity, Average Pressures, Melt Temperatures, and Average Residence Time

(a) Measured Extruder Motor Current Intensity and Average Pressures

Run	Motor Current Intensity (A)	Pressure (MPa) (Average and Standard Deviation)					
		Zone 2	Zone 3	Zone 4	Zone 5	Zone 6	Die
1	21	2.54	7.04	3.49	0.71	0.5–1.0	4.2
		0.25	*0.08*	*0.05*	*0.04*		*0.1*
2	16	2.73	5.57	2.79	0.54	0.6–1.1	3.2
		0.23	*0.05*	*0.04*	*0.01*		*0.1*
3	16	2.48	5.71	2.88	0.58	0.5–1.0	3.7
		0.11	*0.06*	*0.02*	*0.02*		*0.0*
4	18	3.55	6.33	3.01	0.56	0.4–1.0	3.8
		0.18	*0.04*	*0.02*	*0.02*		*0.0*
5	15	2.04	5.45	2.82	0.52	0.2–1.0	3.5
		0.13	*0.05*	*0.02*	*0.02*		*0.1*
6	13	1.66	4.42	2.41	0.51	0.5–1.0	3.0
		0.10	*0.07*	*0.03*	*0.05*		*0.1*
7	21	4.08	7.73	3.68	0.86	0.4–1.0	4.3
		0.09	*0.05*	*0.02*	*0.01*		*0.0*
8	14	0.22	0.10	5.37	0.13	0.0–0.2	3.8
		0.02	*0.00*	*0.11*	*0.03*		*0.1*

(b) Measured Melt Temperatures

Run	Temperature (°C)										
	Measured in the Sample (Average and *Standard Deviation*)						Measured in the Flow (PT) (Average and *Standard Deviation*)				
	Port 2	Port 3	Port 4	Port 5	Port 6	Extrudate	Zone 2	Zone 3	Zone 4	Zone 5	Die
1	145.5	163.7	192.1	203.2	211.3	202.4	185.6	190.4	187	181	—
	5.9	*1.2*	*3.7*	*3.5*	*1.0*	*4.4*	*2.3*	*2.6*	*2*	*1*	
2	145.0	178.8	209.1	232.8	240.5	232.2	223.6	239.2	233	226	—
	2.5	*1.0*	*0.9*	*2.5*	*1.7*	*0.8*	*1.8*	*2.3*	*2*	*3*	
3	148.7	176.0	201.6	221.8	227.0	213.0	206.2	216.5	213	200	212
	1.3	*4.4*	*1.5*	*1.3*	*1.1*	*1.5*	*1.9*	*1.3*	*1*	*8*	*1*
4	140.0	162.8	191.8	212.8	217.5	211.6	205.6	218.0	212	200	210
	4.8	*3.2*	*2.1*	*0.9*	*1.0*	*1.4*	*0.2*	*0.3*	*0*	*1*	*1*
5	148.1	181.9	210.3	229.8	233.2	226.3	209.5	217.1	215	200	214
	4.5	*5.1*	*2.1*	*0.5*	*1.4*	*1.4*	*2.5*	*2.8*	*3*	*1*	*1*
6	149.4	180.2	213.7	227.5	227.5	217.2	207.4	216.3	209	199	208
	2.9	*2.5*	*3.2*	*1.5*	*1.6*	*4.5*	*0.5*	*0.4*	*1*	*8*	*2*
7	129.5	164.3	189.7	214.8	222.2	223.3	206.4	216.3	210	195	214
	5.8	*1.2*	*2.0*	*3.7*	*1.6*	*2.3*	*0.4*	*0.4*	*1*	*3*	*1*
8	—	—	155.6	191.1	210.8	216.9	215.8	217.8	213	201	213
			1.7	*2.6*	*0.8*	*3.2*	*0.5*	*0.5*	*1*	*1*	*1*

(c) Measured Average Residence Time

Run	Average Residence Time (s)		
	Port 4	Port 6	Die Exit
4	23.5	38.7	61.8
5	22.5	33.8	53.5

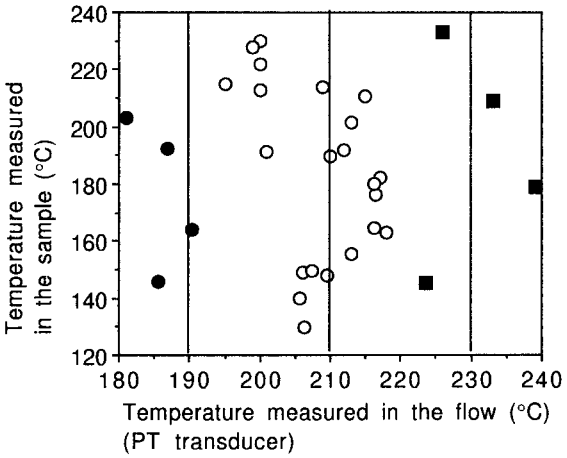

Figure 4 Comparison between temperatures measured in the flow and in the samples (●) T_b = 190°C; (○) T_b = 210°C; (■) T_b = 230°C.

ously, for example, by White and Szydlowski,[17] Meijer and Elemans,[18] or Potente et al.[19] Commercial softwares derived from these studies (e.g., Akroco Twin Screw© or Sigma©) are now available. The Ludovic© software was developed at the Ecole des Mines de Paris–CEMEF and was described in detail elsewhere.[20] It is a global model, based on local 1D approximations, which allows one to compute the evolution of the main-flow parameters (e.g., pressure, temperature, residence time, filling ratio) along the screw profile, between the hopper and the die. Nonisothermal flow conditions, including dissipated power and heat transfer, are assumed. The polymer viscous behavior may be described by a power law or by a Carreau–Yasuda law.

Despite some recent efforts,[22,23] a really satisfactory melting model for twin-screw extrusion is not yet available. Consequently, it was prescribed that melting is instantaneous and that it takes place just prior to the first restrictive element (i.e., a left-handed screw element or a block of kneading discs) exposed to the solid pellets. The global computation follows an iterative scheme, since the calculations proceed backward, starting from an arbitrary initial value of the die exit temperature. This software has been successfully used for many applications, such as the study of starch transformation,[24] of blend morphology evolution,[25] or reactive extrusion.[26,27]

RESULTS AND DISCUSSION

Figure 4 compares, for different processing conditions, the temperatures measured using the two techniques, that is, flush-mounted PT transducers and a manual thermocouple stuck into the collected melt nut. Significant differences of up to 80°C can be observed. Moreover, it appears that the PT transducers, which are not insulated from the barrel wall (which is the most common industrial practice), are largely influenced by the barrel temperature. Such results were also reported by Karwe and Godavarti.[11] Consequently, since flush-mounted PT transducers do not seem capable of monitoring adequately the melt temperature, only the temperatures measured using the sampling devices will be considered in the remainder of this work.

The main results concerning temperature and pressure measurements are depicted in Figures 5–8. For all runs, the temperature increases rapidly in the melting section (ports 2–4). At port 2 (upstream the first block of kneading discs), the

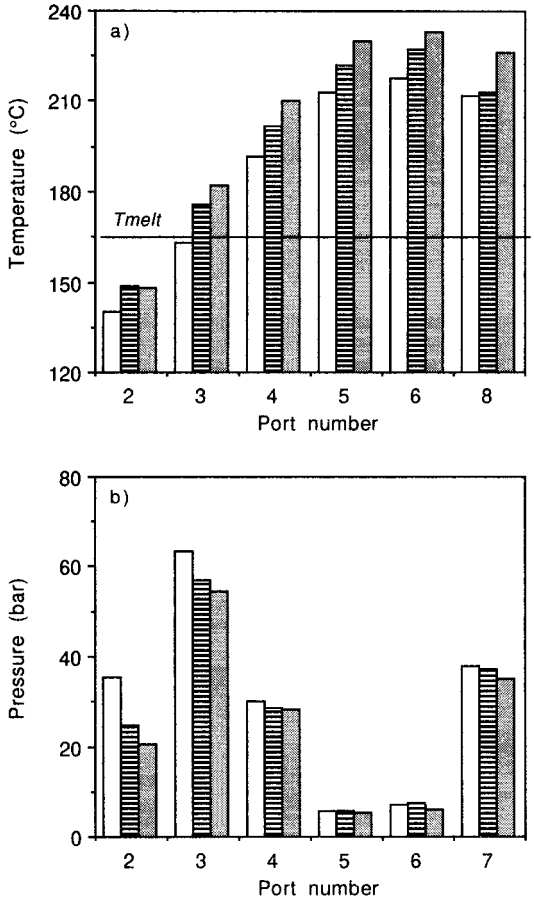

Figure 5 Influence of screw speed on the (a) temperature and (b) pressure measured at the sampling ports (7 corresponds to the die, 8 to the extrudate). Q = 12 kg/h; T_b = 210°C; (□) N = 100 rpm; (▤) N = 150 rpm; (▩) N = 200 rpm.

temperature is lower than the polymer melting temperature, as confirmed by visual examination of the samples collected, which shows that, in most cases, solid granules are still visible at this location. This is demonstrated in Figure 9, which illustrates the evolution of plastication along the barrel for the various runs, as inferred from the analysis of the samples collected. Further downstream, the temperature profile is influenced mainly by the screw speed, feed rate, and barrel temperature. Melt temperature increases with increasing rotation speed [Fig. 5(a)] due to viscous dissipation, with a decreasing feed rate [Fig. 6(a)] due to higher specific energy and with an increasing barrel temperature [Fig. 7(a)] due to more heat conduction. Thus, all the processing parameters have a clear influence on the temperature profile. Moreover, when using the same processing conditions [Figs. 8(a) and 9], melting occurs earlier in screw A (port 3) than in screw B (port 5). In screw B, solid granules are present at ports 2 and 3, that is, at the screw elements preceding the left-handed element. Here, the majority of the material melts, but some granules are still visible. Full melting in screw B is only achieved in the block of right-handed kneading discs (port 5). Further downstream, the temperature increase rate diminishes since the screw profile is less severe, although the outlet temperatures of both screws are very similar.

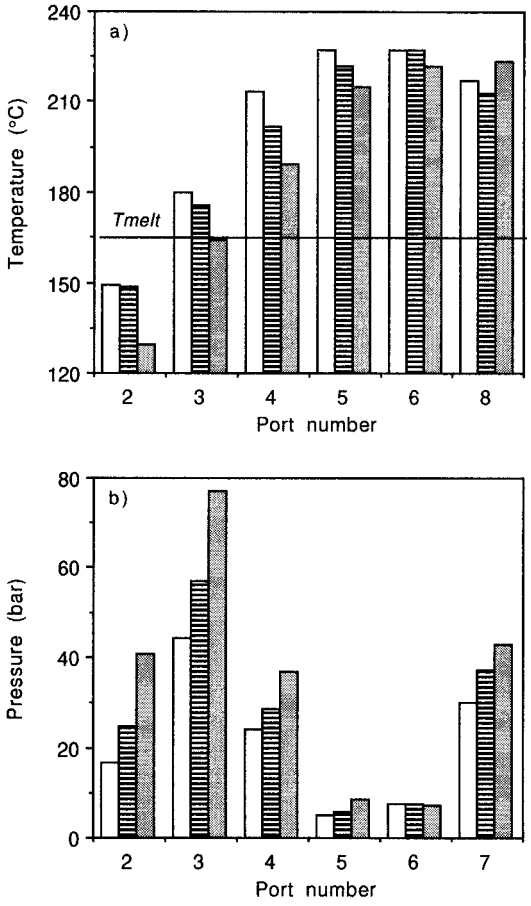

Figure 6 Influence of feed rate on (a) temperature and (b) pressure measured at the sampling ports (7 corresponds to the die, 8 to the extrudate). N = 150 rpm; T_b = 210°C; (□) Q = 6 kg/h; (▤) Q = 12 kg/h; (■) Q = 18 kg/h.

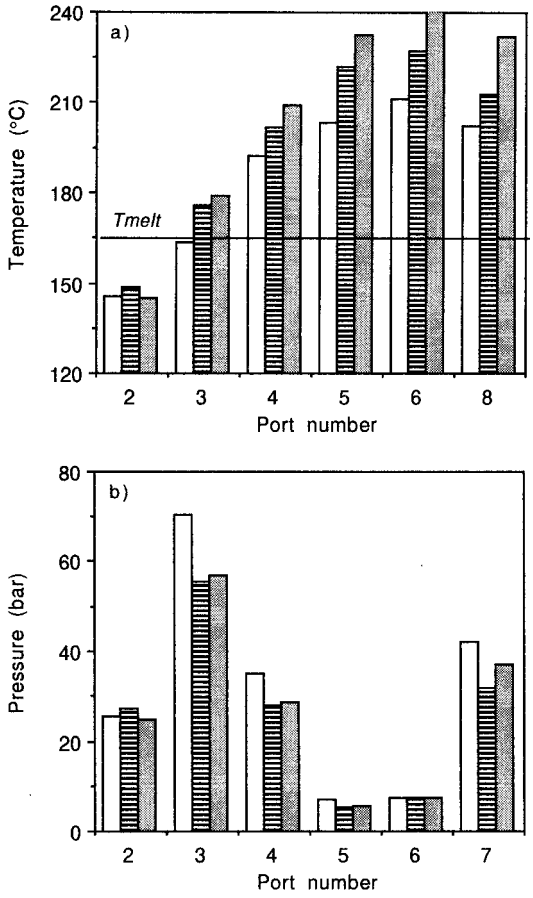

Figure 7 Influence of barrel temperature on (a) temperature and (b) pressure, measured at the sampling ports (7 corresponds to the die, 8 to the extrudate). N = 150 rpm; Q = 12 kg/h; (□) T_b = 190°C; (▤) T_b = 210°C; (■) T_b = 230°C.

For screw A, the pressure reaches a maximum of 4.4–7.7 MPa at port 3 (before the left-handed element), depending on the operating conditions. This pressure increases sharply with increasing feed rate [Fig. 6(b)] or decreasing barrel temperature [Fig. 7(b)] and decreases slightly with increasing screw speed [Fig. 5(b)]. Conversely, the pressure in the mixing elements (ports 5 and 6) is

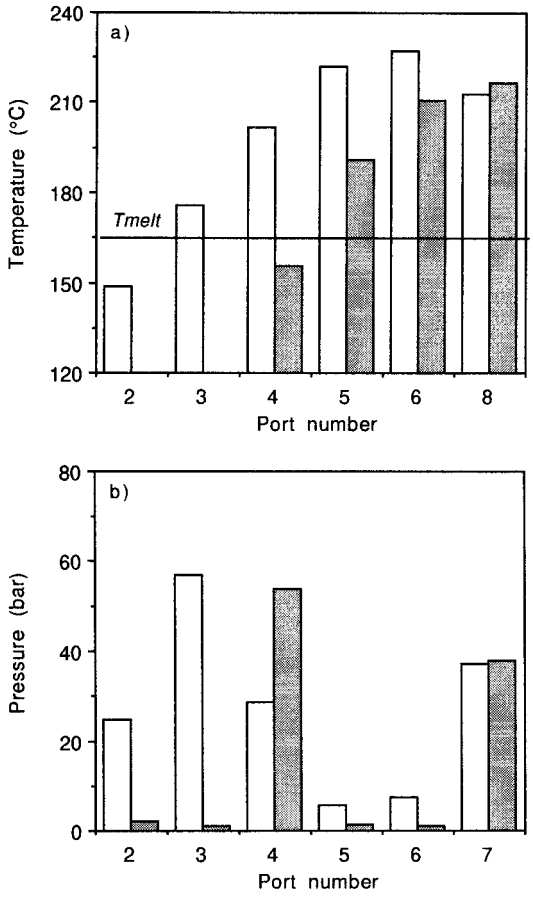

Figure 8 Influence of screw profile on the (a) temperature and (b) pressure measured at the sampling ports (7 corresponds to the die, 8 to the extrudate). N = 150 rpm; Q = 12 kg/h; T_b = 210°C; (□) screw A; (■) screw B.

quite insensitive to variations in the processing conditions and is characterized by low values, ranging between 0.4 and 0.9 MPa. These values are in agreement with data previously published in the literature.[8,9] As expected, the pressure profile for screw B is significantly different [Fig. 8(b)]. It is also characterized by a peak in the left-handed element (port 4), but the pressures in the kneading discs are much lower than for screw A, as we have positive (60°) or neutral (90°) staggering angles. Die pressures are quite identical, as the final temperatures and throughputs are similar.

The average residence times shown in Table IV(c) clarify the influence of the screw speed. An increase in the value of this parameter (from 100 to 200 rpm) promotes a decrease in the average residence time in all the locations considered, since the material advances with a higher speed in partially filled sections.[28]

The various runs of Table III were computed with Ludovic© using a heat-transfer coefficient evaluated as 1500 W m^{-2} $°C^{-1}$. Figure 10 presents, as an example, the predicted and experimental pressure and temperature profiles for run 3, corresponding to the central experimental conditions (Q = 12 kg/h, N = 150 rpm, T_b = 210°C). The screws are partially filled, with only the die and the restrictive elements being under pressure. The global agreement between computation and experiments is good. The order of magnitude of the pressures is well described by the model. The melt temperature increases as the material flows through the mixing elements due to viscous dissipation and decreases in the conveying sections due to heat transfer toward the colder barrel. The agreement between the predictions and the experiments is poorer in the first part of the extruder, where the temperature is significantly overestimated. In fact, samples extracted from the collecting devices evidenced the survival of granules up to port 3 (axial position: 0.62 m, see Fig. 1), as illustrated in Figure 9. This means that melting is not instantaneous as assumed theoretically, but develops along the first kneading block, inducing a progressive increase in the average material temperature. Prescribing that full melting occurs between ports 3 and 4 produces very good agreement with the experimental data (Fig. 11). Therefore, in the remainder of this work, all computations will be carried out assuming the experimentally observed location of the onset of melting.

The influence of the barrel temperature can be observed in Figure 12. The extrudate temperature is highly dependent on this variable, which demonstrates the importance of heat transfer in the overall process. The results also show that, in industrial practice, even when the exit temperature seems to exhibit the correct values, it is possible that, at various locations along the screw profile (depending on the local screw configuration), hot spots occur which could lead to polymer degradation problems. Again, the simulation provides a good description of the experiments.

Screw speed seems to have a stronger influence on the process than does the feed rate, as shown in Figure 13. For this particular case, it seems that the former only influences viscous dissipation, while the latter affects both viscous dissipation and heat transfer, which have conflicting effects. This sensitivity is correctly described by the model. Again, temperatures reached inside the

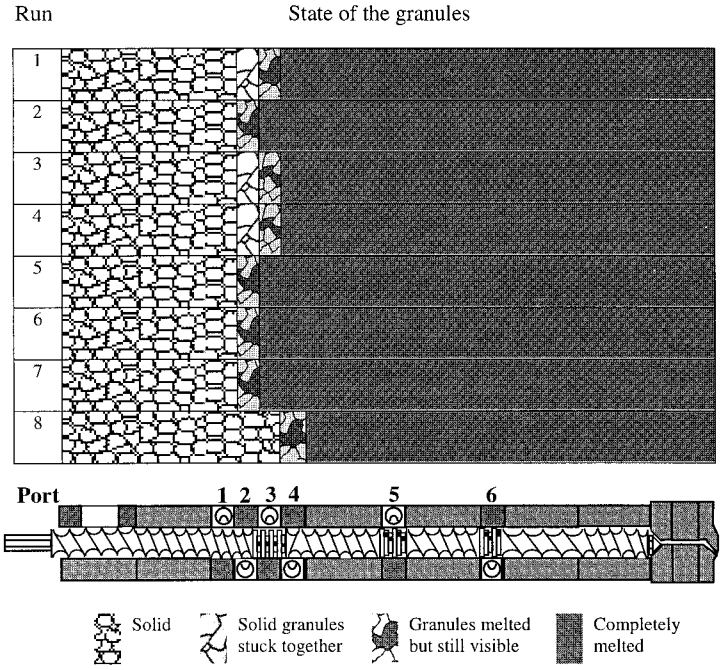

Figure 9 Evolution of plastication (experimental data).

extruder may be 30°C higher than the ones measured at the die exit.

Residence time and residence time distribution are other important parameters in twin-screw extrusion, particularly when chemical reactions occur inside the machine. Since the Ludovic© software is based on simple 1D approximations, it is not possible to compute a residence time distribution. However, the time spent in each successive screw element provides an estimation of the local average residence time, which can then be compared with the experimental mean values obtained for ports 4 and 6 and at the die exit [see Table IV(c)]. Figure 14 shows that the software is able to capture adequately this information, that is, the cumulative residence times along the screw and die outlet are correctly estimated.

The results obtained with the second screw profile [denoted B, see Fig. 2(b)] are shown in Figure 15. As expected, this profile is less severe than is screw A (see also Fig. 9). The left-handed element and the die are the only filled parts of the machine. As for screw A, the pressure evolution is correctly predicted, whereas the temperature is largely overestimated. Again, the original assumption that melting takes place in front of the left-handed element proves to be incorrect (see Fig. 9). During the experiment, partially melted granules were collected at port 4 (axial position: 0.58 m), that is, while the material was flowing

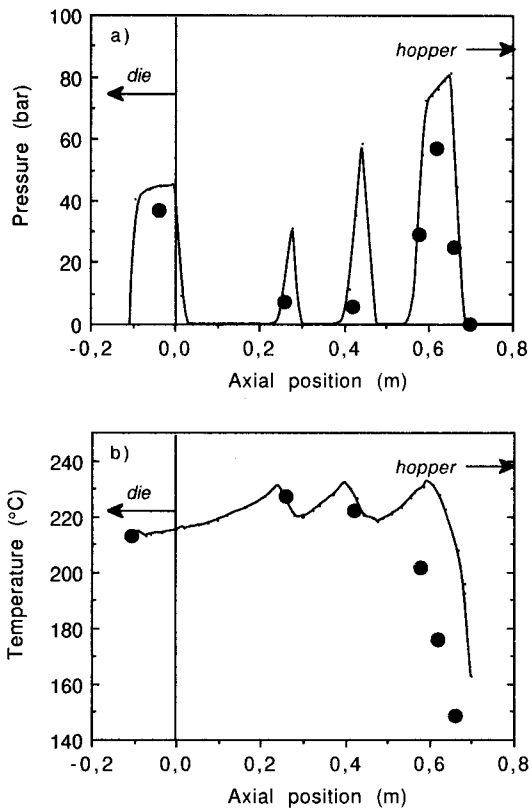

Figure 10 Evolution of the computed (a) pressure and (b) temperature along the screw profile. Q = 12 kg/h; N = 150 rpm; T_b = 210°C; symbols (●) are experimental values measured at the ports.

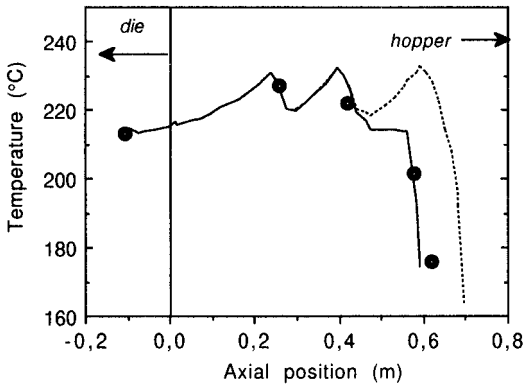

Figure 11 Comparison between (●) measured and computed temperature profiles Q = 12 kg/h; N = 150 rpm; T_b = 210°C; (full line) melting at experimental location; (dotted line) melting in front of the first restrictive element.

through the left-handed element. As before, when setting the correct location of melting in the simulation, the predictions improve substantially, as illustrated in Figure 16. The need for inserting a more precise melting model in the software is thus confirmed and is currently in progress.[29]

Finally, Figures 17 and 18 present a general comparison between computed and measured parameters for the various runs of Table III. The predicted temperatures at different screw locations are within ±10% of the measured values. The pressures seem slightly overestimated, but this could simply be due to the very sharp gradients observed (see, e.g., Fig. 10), which originate large pressure differences even for small errors in the axial location of the transducer. The specific energy (derived from the motor current) is also

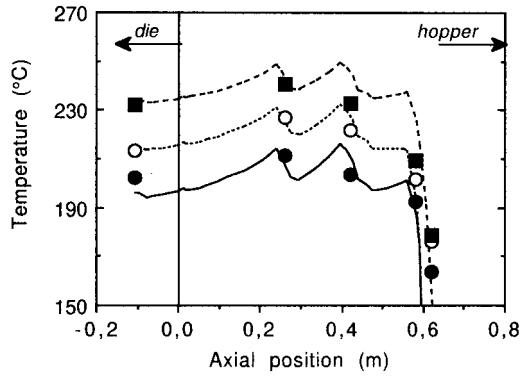

Figure 12 Comparison between measured and computed temperature profiles for different values of barrel temperature. Q = 12 kg/h; N = 150 rpm; (●) T_b = 190°C; (○) T_b = 210°C; (■) T_b = 230°C.

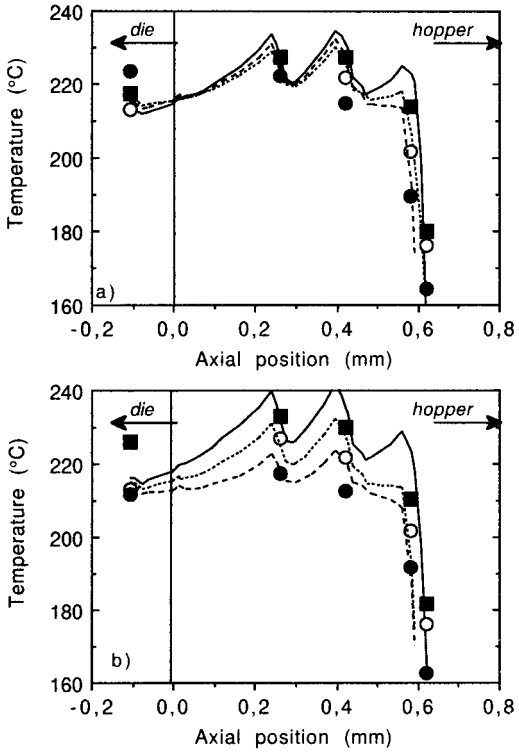

Figure 13 Comparison between measured and computed temperature profiles for different values of (a) feed rate [N = 150 rpm; (●) Q = 6 kg/h; (□) Q = 12 kg/h; (●) Q = 18 kg/h] and (b) screw speed [Q = 12 kg/h; (●) N = 100 rpm; (□) N = 150 rpm; (■) N = 200 rpm].

correctly predicted by the model (Fig. 18). Whatever the processing conditions and the screw configuration, Ludovic© software seems able to pro-

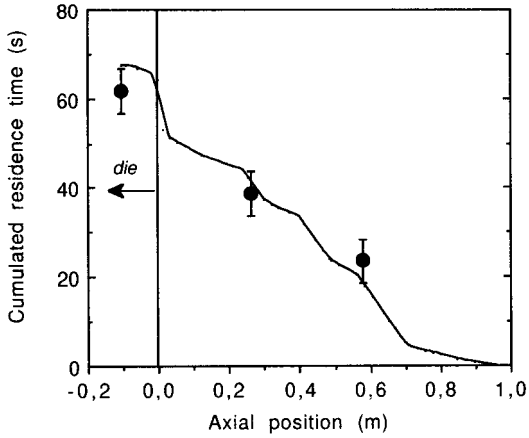

Figure 14 Comparison between (●) measured and computed cumulative residence time. Run 4; Q = 12 kg/h; N = 100 rpm; T_b = 210°C.

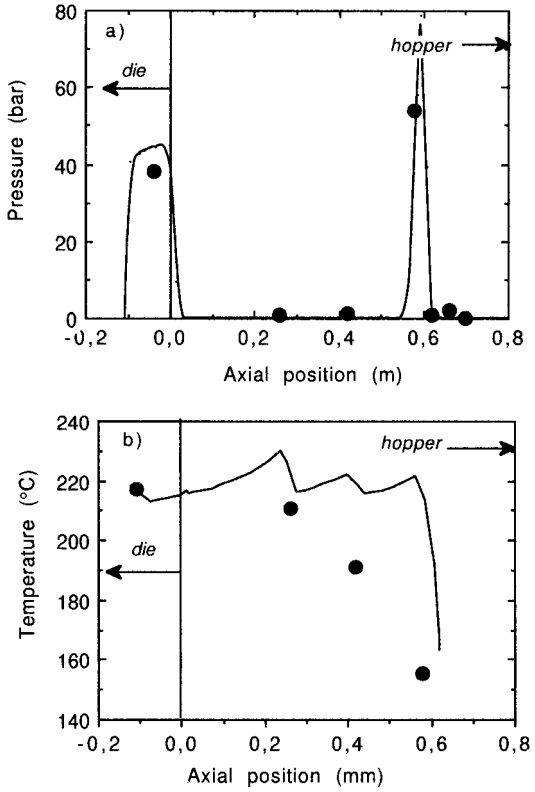

Figure 15 Evolution of the computed (a) pressure and (b) temperature along the second screw profile B. Q = 12 kg/h; N = 150 rpm; T_b = 210°C. Symbols (●) are experimental values measured at the ports.

vide a correct estimation of the main thermomechanical process parameters. In practice, this makes it useful for optimizing screw profiles or for solving scale-up problems.

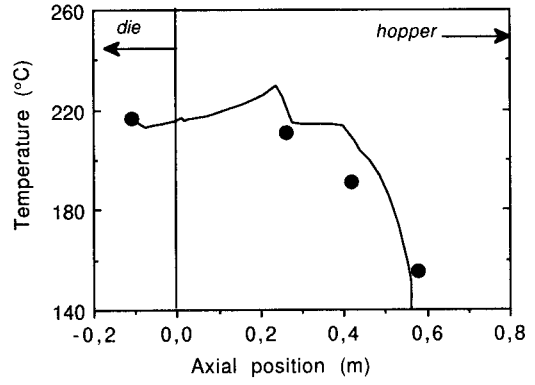

Figure 16 Comparison between (●) measured and computed temperature profiles when melting is assumed at the end of the left-handed element. Q = 12 kg/h; N = 150 rpm; T_b = 210°C.

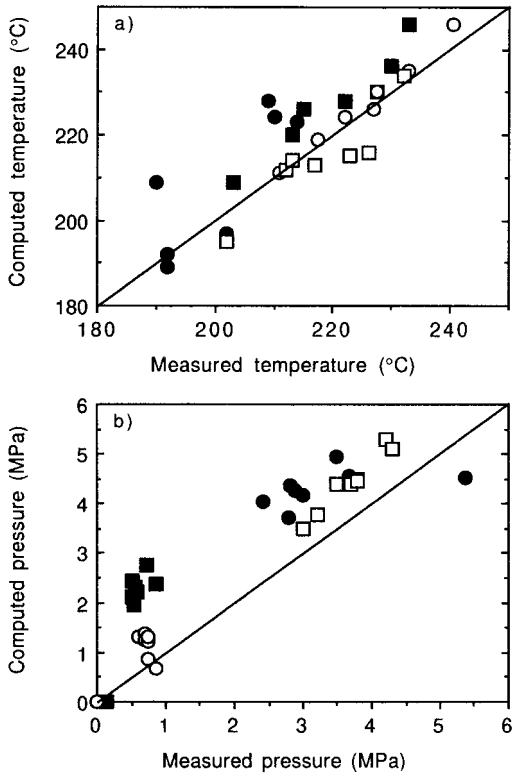

Figure 17 Comparison between measured and computed (a) temperatures and, (b) pressures: (■) port 4; (●) port 5; (○) port 6; (□) die.

CONCLUSIONS

Experiments using novel sampling devices and flow modeling were used as complementary powerful tools for a better understanding of the twin-screw extrusion process. It was confirmed that the use of flush-mounted PT transducers does not guarantee an adequate temperature measure-

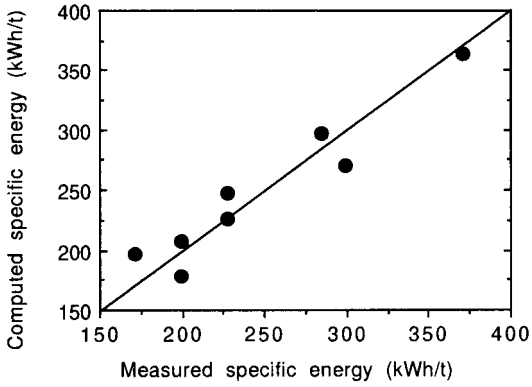

Figure 18 Comparison between measured and computed specific energy.

ment. Generally, the extrusion experiments carried out validated the theoretical model, which, in turn, is capable of providing additional information on local parameters such as degree of filling, shear rate, deformation, and viscosity, which is difficult to obtain in practice. Finally, it has been shown that a better melting model should be developed, if the predictions of the software are to be improved.

This work was carried out through a French–Portuguese collaboration between École des Mines de Paris–CEMEF and the University of Minho, Department of Polymer Engineering. Financial support from ICCTI and Ambassade de France, both in Portugal, is greatly acknowledged.

REFERENCES

1. White, J. L. Twin Screw Extrusion, Technology and Principles; Hanser: Munich, 1990.
2. Xanthos, M. Reactive Extrusion, Principles and Practice; Hanser: Munich, 1992.
3. Hu, G. H.; Kadri, I.; Picot, C. Polym Eng Sci 1999, 39, 930.
4. Oberlehener, J.; Cassagnau, P.; Michel, A. Chem Eng Sci 1994, 49, 3897.
5. Kim, P. J.; White, J. L. Int Polym Proc 1994, 9, 108.
6. Chalamet, Y.; Taha, M. Polym Eng Sci 1999, 39, 347.
7. Chen, T.; Patterson, W. I.; Dealy, J. M. Int Polym Proc 1995, 10, 3.
8. Huneault, M. SPE ANTEC Tech Pap 1997, 100.
9. McCullough, T. W.; Hilton, B. T. SPE ANTEC Tech Pap 1993, 3372.
10. Nietsch, T.; Cassagnau, P.; Michel, A. Int Polym Proc 1997, 12, 307.
11. Karwe, M. V.; Godavarti, S. J Food Sci 1997, 62, 367.
12. Machado, A. V.; Covas, J. A.; van Duin, M. J Appl Polym Sci 1999, 71, 135.
13. Kajiwara, T.; Nagashima, Y.; Nakano, Y.; Funatsu, K. Polym Eng Sci 1998, 36, 275.
14. Cheng, H. F.; Manas-Zloczower, I. Polym Eng Sci 1998, 38, 926.
15. Ishikawa, T.; Kihara, S. I.; Funatsu, K. Polym Eng Sci 2000, 40, 357.
16. Cheng, H. F.; Manas-Zloczower, I. Polym Eng Sci 1997, 37, 1082.
17. White, J. L.; Szydlowski, W. Adv Polym Tech 1987, 7, 419.
18. Meijer, H. E. H.; Elemans, P. H. M. Polym Eng Sci 1988, 28, 275.
19. Potente, H.; Ansahl, J.; Klarholtz, B. Int Polym Proc 1994, 9, 11.
20. Vergnes, B.; Della Valle, G.; Delamare, L. Polym Eng Sci 1998, 38, 1781.
21. Wolf, D.; White, D. H. AIChE J 1976, 22, 122.
22. Potente, H.; Melish, U. Int Polym Proc 1996, 11, 101.
23. Bawiskar, S.; White, J. L. Polym Eng Sci 1998, 38, 727.
24. Della Valle, G.; Barrès, C.; Plewa, J.; Tayeb, J.; Vergnes, B. J Food Eng 1993, 19, 1.
25. Delamare, L.; Vergnes, B. Polym Eng Sci 1996, 36, 1685.
26. Berzin, F.; Vergnes, B. Int Polym Proc 1998, 13, 13.
27. Berzin, F.; Vergnes, B.; Dufossé, P.; Delamare, L. Polym Eng Sci 2000, 40, 344.
28. Carneiro, O. S.; Caldeira, G.; Covas, J. A. Mat Proc Tech, in press.
29. Vergnes, B.; Delecour, M. L.; Souveton, G.; Bouvier, J. M. In PPS-15 Annual Meeting, 's Hertogenbosch, 1999.